Sucrose Efflux Mediated by SWEET Proteins as a Key Step for Phloem Transport

Li-Qing Chen, *et al.*

Science **335**, 207 (2012);
DOI: 10.1126/science.1213351

References and Notes

1. R. Criegee, *Angew. Chem. Int. Ed. Engl.* **14**, 745 (1975).
2. J. G. Calvert *et al*., *The Mechanisms of Atmospheric Oxidation of the Alkenes* (Oxford Univ. Press, New York, 2000).
3. D. E. Heard *et al*., *Geophys. Res. Lett.* **31**, L18112 (2004).
4. R. M. Harrison *et al*., *Sci. Total Environ.* **360**, 5 (2006).
5. K. J. Heaton, R. L. Sleighter, P. G. Hatcher, W. A. Hall 4th, M. V. Johnston, *Environ. Sci. Technol.* **43**, 7797 (2009).
6. J. H. Kroll, J. H. Seinfeld, *Atmos. Environ.* **42**, 3593 (2008).
7. D. Johnson, G. Marston, *Chem. Soc. Rev.* **37**, 699 (2008).
8. S. Hatakeyama, H. Akimoto, *Res. Chem. Intermed.* **20**, 503 (1994).
9. M. S. Alam *et al*., *Phys. Chem. Chem. Phys.* **13**, 11002 (2011).
10. A. A. Presto, N. M. Donahue, *J. Phys. Chem. A* **108**, 9096 (2004).
11. N. M. Donahue, G. T. Drozd, S. A. Epstein, A. A. Presto, J. H. Kroll, *Phys. Chem. Chem. Phys.* **13**, 10848 (2011).
12. J. D. Fenske, A. S. Hasson, A. W. Ho, S. E. Paulson, *J. Phys. Chem. A* **104**, 9921 (2000).
13. C. A. Taatjes *et al*., *J. Am. Chem. Soc.* **130**, 11883 (2008).
14. L. J. Carpenter, *Chem. Rev.* **103**, 4953 (2003).
15. A. J. Eskola, D. Wojcik-Pastuszka, E. Ratajczak, R. S. Timonen, *Phys. Chem. Chem. Phys.* **8**, 1416 (2006).
16. M. T. Nguyen, T. L. Nguyen, V. T. Ngan, H. M. T. Nguyen, *Chem. Phys. Lett.* **448**, 183 (2007).
17. T. A. Cool, J. Wang, K. Nakajima, C. A. Taatjes, A. McIlroy, *Int. J. Mass Spectrom.* **247**, 18 (2005).
18. M. Olzmann, E. Kraka, D. Cremer, R. Gutbrod, S. Andersson, *J. Phys. Chem. A* **101**, 9421 (1997).
19. J. H. Kroll, J. S. Clarke, N. M. Donahue, J. G. Anderson, K. L. Demerjian, *J. Phys. Chem. A* **105**, 1554 (2001).
20. T. J. Gravestock, M. A. Blitz, W. J. Bloss, D. E. Heard, *ChemPhysChem* **11**, 3928 (2010).
21. T. J. Dillon, M. E. Tucceri, R. Sander, J. N. Crowley, *Phys. Chem. Chem. Phys.* **10**, 1540 (2008).
22. R. A. Cox, S. A. Penkett, *Nature* **230**, 321 (1971).
23. T. Kurtén, J. R. Lane, S. Jørgensen, H. G. Kjaergaard, *J. Phys. Chem. A* **115**, 8669 (2011).
24. S. Gäb, E. Hellpointner, W. V. Turner, F. Korte, *Nature* **316**, 535 (1985).
25. A. S. Hasson *et al*., *J. Phys. Chem. A* **107**, 6176 (2003).
26. A. T. Archibald *et al*., *Atmos. Chem. Phys.* **10**, 8097 (2010).
27. F. Paulot *et al*., *Atmos. Chem. Phys.* **11**, 1989 (2011).
28. C. D. O'Dowd *et al*., *Nature* **417**, 632 (2002).
29. J. Sehested, T. Ellermann, O. J. Nielsen, *Int. J. Chem. Kinet.* **26**, 259 (1994).
30. W. Klemperer, V. Vaida, *Proc. Natl. Acad. Sci. U.S.A.* **103**, 10584 (2006).
31. S. Aloisio, J. S. Francisco, *Acc. Chem. Res.* **33**, 825 (2000).

Acknowledgments: Additional pseudo–first-order rate constants and spectroscopic data underpinning this work are presented in the SOM. This work is supported by the Division of Chemical Sciences, Geosciences, and Biosciences, the Office of Basic Energy Sciences, the U.S. Department of Energy. D.E.S. and C.J.P. thank Natural Environment Research Council for funding. The Advanced Light Source is supported by the Director, Office of Science, Office of Basic Energy Sciences, Materials Sciences Division, of the U.S. Department of Energy under contract DE-AC02-05CH11231 at Lawrence Berkeley National Laboratory. Sandia is a multiprogram laboratory operated by Sandia Corporation, a Lockheed Martin company, for the National Nuclear Security Administration under contract DE-AC04-94-AL85000. We thank A. Eskola (Helsinki) for drawing our attention to the reaction of CH_2I with O_2, H. Johnsen (Sandia) for technical support of this experiment, and H. Huang, J. Zádor, and L. Sheps (Sandia) for discussions on data analysis. The experiments were conceived by C.A.T., C.J.P., and D.E.S. and designed and carried out by O.W., J.D.S., C.A.T., and D.L.O., with assistance from S.S.V. All authors participated in the data analysis and interpretation and contributed to the manuscript.

Supporting Online Material

www.sciencemag.org/cgi/content/full/335/6065/204/DC1
Materials and Methods
Figs. S1 to S14
Tables S1 and S2
References (*32*–*51*)

26 August 2011; accepted 18 November 2011
10.1126/science.1213229

Sucrose Efflux Mediated by SWEET Proteins as a Key Step for Phloem Transport

Li-Qing Chen,[1]* Xiao-Qing Qu,[1,2]* Bi-Huei Hou,[1] Davide Sosso,[1] Sonia Osorio,[3] Alisdair R. Fernie,[3] Wolf B. Frommer[1]†

Plants transport fixed carbon predominantly as sucrose, which is produced in mesophyll cells and imported into phloem cells for translocation throughout the plant. It is not known how sucrose migrates from sites of synthesis in the mesophyll to the phloem, or which cells mediate efflux into the apoplasm as a prerequisite for phloem loading by the SUT sucrose–H^+ (proton) cotransporters. Using optical sucrose sensors, we identified a subfamily of SWEET sucrose efflux transporters. AtSWEET11 and 12 localize to the plasma membrane of the phloem. Mutant plants carrying insertions in *AtSWEET11* and *12* are defective in phloem loading, thus revealing a two-step mechanism of SWEET-mediated export from parenchyma cells feeding H^+-coupled import into the sieve element–companion cell complex. We discuss how restriction of intercellular transport to the interface of adjacent phloem cells may be an effective mechanism to limit the availability of photosynthetic carbon in the leaf apoplasm in order to prevent pathogen infections.

Breeding has led to marked increases in crop yield. Increased yield potential has mainly been attributed to improvements in allocation efficiency, defined as the amount of total biomass allocated into harvestable organs (*1*, *2*). Despite the critical importance of sucrose translocation in this process, we do not understand mechanistically how changes in translocation efficiency may have contributed to an increase in harvestable products. Allocation of photoassimilates in plants is conducted by transport of sucrose from the photosynthetic "sources" (predominantly leaves) to the heterotrophic "sinks" (meristems, roots, flowers, and seeds) (*3*–*5*). Sucrose, the predominant transport form of sugars in many plant species [see (*6*) for an overview of the different sugars and translocation mechanisms], is produced in leaf mesophyll cells, particularly in the palisade parenchyma of dicots and the bundle sheath of monocots.

In apoplasmic loaders, sucrose is loaded into the sieve element–companion cell complex (SE/CC) in the phloem by the sucrose-H^+ cotransporter SUT1 (named SUC2 in *Arabidopsis*) from the apoplasm (cell wall space) (*7*–*11*). However, sucrose must effuse from inside the cell into the cell wall, either directly from mesophyll cells (after which it travels to the phloem in the apoplasm) or from cells closer to the site of loading (having traveled cell-to-cell through plasmodesmata). Both the site and the mechanism of sucrose efflux remain to be elucidated, although it has been argued that a site in the vicinity of the site of phloem loading is most probable (*4*, *5*).

We identified proteins that can transport sucrose across the plasma membrane: AtSWEET10 to 15 in *Arabidopsis* and OsSWEET11 and 14 in rice (*Oryza sativa*). We found that *AtSWEET11* and *12* are expressed in phloem cells, and that inhibition by mutation reduces leaf assimilate exudation and leads to increased sugar accumulation in leaves. Thus, apoplasmic phloem loading occurs in a two-step model: Sucrose exported by SWEETs from phloem parenchyma cells feeds the secondary active proton-coupled sucrose transporter SUT1 in the SE/CC.

The sucrose efflux transporters were identified by means of a Förster resonance energy transfer (FRET) sensor-based screen. Because humans do not seem to possess sucrose transporters, we reasoned that human cell lines should lack endogenous sucrose transport activity and should thus represent a suitable functional expression system for heterologous sucrose transporters. A preliminary set of ~50 candidate genes encoding membrane proteins with unknown function as well as members of the recently identified SWEET glucose effluxer family (*12*) were coexpressed with the FRET sucrose sensor FLIPsuc90μΔ1V (*13*) in human embryonic kidney (HEK) 293T cells. AtSWEET10 to 15, which all belong to clade III of the AtSWEET family

[1]Carnegie Institution for Science, 260 Panama Street, Stanford, CA 94305, USA. [2]Key Laboratory of Plant and Soil Interactions, College of Resources and Environmental Sciences, China Agricultural University, 100193 Beijing, China. [3]Max-Planck-Institut für Molekulare Pflanzenphysiologie, Am Mühlenberg 1, 14476 Potsdam, Germany.

*These authors contributed equally to this work.
†To whom correspondence should be addressed. E-mail: wfrommer@stanford.edu

(*12*), enabled HEK293T cells to accumulate sucrose, as detected by a negative ratio change in sensor output (Fig. 1A). To corroborate these findings, we tested the clade III orthologs OsSWEET11 and 14 from rice (Fig. 1B) and found that they also transport sucrose. By contrast, proteins from the other SWEET clades did not show detectable sucrose uptake into HEK293T cells (Fig. 1A). Clade III SWEETs showed preferential transport activity for sucrose over glucose and did not appear to transport maltose (Fig. 1C and fig. S2). The ability of clade III SWEETs to export sucrose was shown by time-dependent efflux of [^{14}C]sucrose injected into *Xenopus* oocytes (Fig. 1D and fig. S2D) and was further supported by the reversibility of sucrose accumulation as measured by optical sensors in mammalian cells (Fig. 1E and fig. S3). SWEETs function as low-affinity sucrose transporters (affinity constant K_m for sucrose uptake by AtSWEET12 was ~70 mM, K_m for efflux was >10 mM; Fig. 1F and fig. S4, A to C). The largely pH-independent transport activity supports a uniport mechanism (fig. S4D). The observed transport characteristics are compatible with those of the low-affinity components for sucrose transport detected in vivo (*14*, *15*).

AtSWEET11 and *12* are highly expressed in leaves [microarray data and translatome data (*16*, *17*) (figs. S5A and S6)] and were found to be coexpressed with genes involved in sucrose biosynthesis and phloem loading (e.g., sucrose phosphate synthase, *SUC2*, and *AHA3*; fig. S5, B and C). The tissue-specific expression and cellular localization of AtSWEET11 and 12 and the phenotypes of *sweet* mutants were analyzed to determine the physiological role of the sucrose transporters.

AtSWEET11 and 12 are close paralogs, with 88% similarity at the amino acid level. Lines carrying single T-DNA (transfer DNA; *Agrobacterium tumefaciens*) insertions (fig. S7) in the *AtSWEET11* and *12* loci did not show any obvious altered morphological phenotype when compared to the wild-type Col-0 or wild-type siblings segregated from the same mutant populations. However, at higher light levels, the double mutant line was smaller relative to wild-type controls (20 to 35% reduction in rosette diameter depending on light conditions; Fig. 2A and fig. S8) and contained elevated starch levels at the end of the diurnal dark period (Fig. 2, B and C). Moreover, mature leaves of the double mutant contained higher sucrose levels both at the end of the light period and the end of the dark period (Fig. 2D). Leaves also accumulated higher levels of hexoses, as also observed in plants exposed to sucrose (*18*) or plants in which phloem loading has been blocked (*9*, *19*). Accumulation of free sugars is expected to lead to down-regulation of photosynthesis through sugar signaling networks (*20*). The starch accumulation phenotype was partially complemented by expression of either *AtSWEET11* or *12* under their respective promoters in the double mutant (fig. S9). Together, these data indicate an impaired ability of the mutants to export sucrose from the leaves. Direct [$^{14}CO_2$]-labeling experiments indicated that under low light conditions (in which the double mutant did not accumulate high starch levels; fig. S10), the double mutant exported ~50% of fixed ^{14}C relative to controls (Fig. 2E). It is noteworthy that the mutant was affected with respect to leaf size, photosynthetic capacity, and steady-state sugar levels; thus, the apparent efflux rates may be compounded by these parameters.

Reduced efflux of sugars from leaves is expected to lead to reduced translocation of photoassimilates to the roots, thus negatively affecting

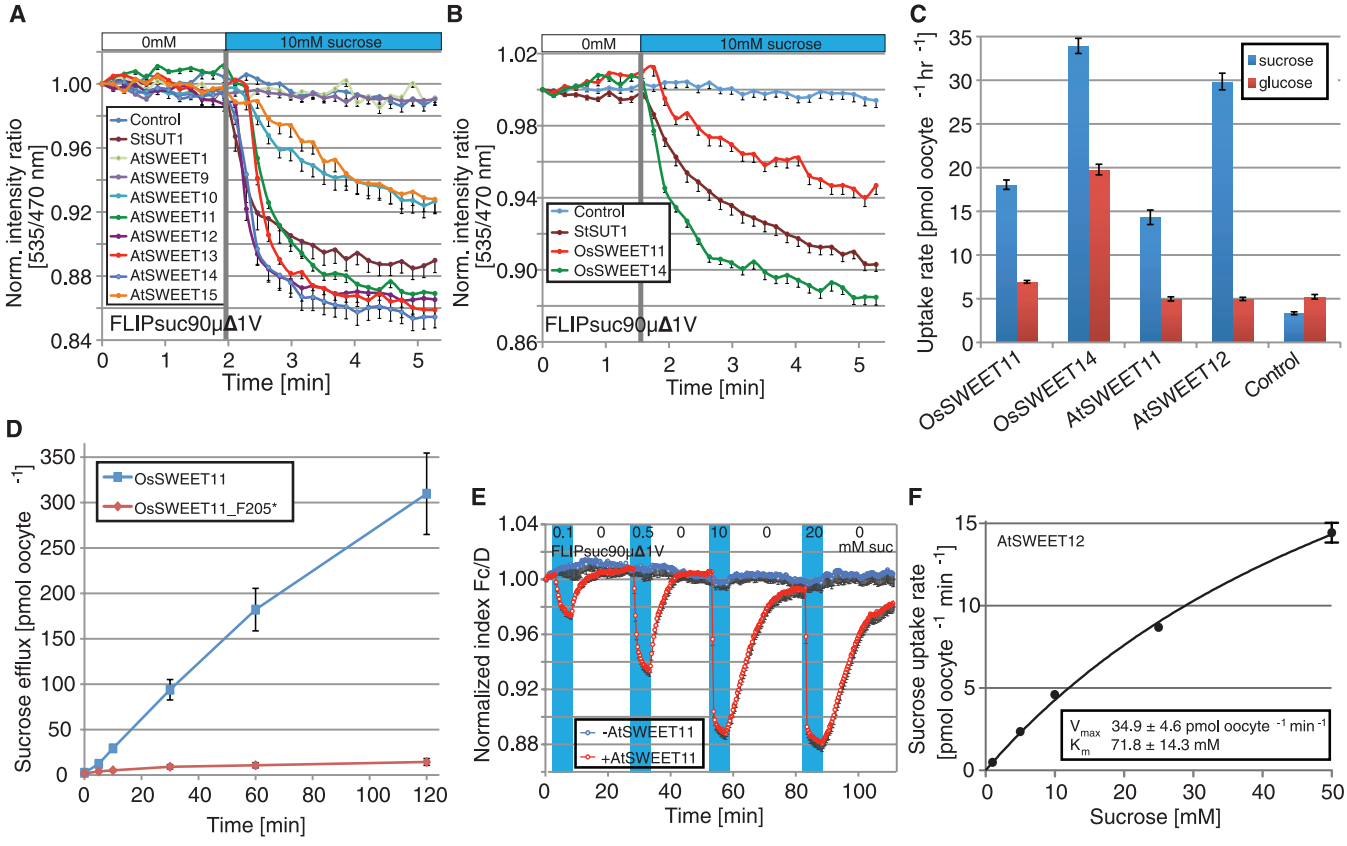

Fig. 1. Identification of sucrose transporters. (**A** and **B**) HEK293T cell–FRET sensor uptake assay. (A) Of ~50 membrane protein genes tested, AtSWEET10 to 15 showed sucrose influx as measured with the sucrose sensor FLIPsuc90μΔ1V; HEK293T cells transfected with sensor only ("control") or the sensor and the H^+/sucrose cotransporter StSUT1 served as controls (fig. S1) (*7*) (±SEM, $n \geq 11$). (B) The rice transporters OsSWEET11 and 14 mediate sucrose transport in HEK293T cells (±SEM, $n \geq 11$). (**C**) Oocyte uptake assay: OsSWEET11 and 14 and AtSWEET11 and 12 mediate [^{14}C]sucrose uptake (1 mM sucrose; ±SEM, $n \geq 7$). (**D**) Oocyte efflux assay: [^{14}C]sucrose efflux by OsSWEET11 in *Xenopus* oocytes injected with 50 nl of a solution containing 50 mM [^{14}C]sucrose; the truncated version OsSWEET11_F205* served as control (±SEM, $n \geq 7$). (**E**) HEK293T cell–FRET sensor transport assay: Reversible accumulation of sucrose in HEK293T cells by AtSWEET11 (±SEM, $n \geq 10$; Fc/D, FRET index). (**F**) Oocyte uptake assay: Kinetics of AtSWEET12 for sucrose uptake in *Xenopus* oocytes (±SEM, $n \geq 14$).

root growth and the ability to acquire mineral nutrients (*9*, *10*). When germinated in the light on sugar-free media, *atsweet11;12* mutants exhibited reduced root length (Fig. 2, F and G). Addition of sucrose to the media rescued the root growth deficiency of *atsweet11;12* mutants (Fig. 2, F and G). A similar sucrose-dependent root growth deficiency has also been observed for the *Arabidopsis* sucrose/H^+ cotransporter *suc2* mutant (*11*). Both the *suc2* and the *atsweet11;12* mutants are apparently able to acquire sucrose or sucrose-derived hexoses from the medium to restore root growth that had been restricted by a carbohydrate deficiency.

The growth phenotype for *atsweet11;12* is not as severely affected as described previously for the *suc2* mutant (*9*–*11*). The *Arabidopsis* genome encodes several SWEET paralogs, including the closely related transporters AtSWEET10, 13, 14, and 15, which we show here to function as sucrose transporters. Quantitative polymerase chain reaction analyses showed that *AtSWEET13*, which is typically expressed at low levels in leaves, is induced by a factor of ~16 in the *atsweet11;12* double mutant (fig. S11). Thus, in contrast to the secondary active SE/CC loaders SUT1/SUC2, SWEETs function as redundant elements of phloem loading. It is noteworthy that *ossweet14* rice mutants display stunted growth, possibly as a result of reduced sugar efflux from leaves as well (*21*).

Taken together, the data indicate that clade III SWEETs are involved in export of sucrose and are responsible for the previously undescribed first step in phloem loading. The efflux of sucrose to the apoplasm could theoretically occur directly at the site of production in mesophyll cells, from bundle sheath cells, or from phloem parenchyma cells. Localization of *AtSWEET11* and *12* driven by their native promoters, as translational enhanced green fluorescent protein (eGFP) or GUS fusions, revealed that both proteins are present in the vascular tissue including minor and major veins, which in *Arabidopsis* are considered "to participate in phloem loading" (*22*) (Fig. 3, A to D, and fig. S12). The subcellular localization of eGFP-tagged AtSWEET11 and 12 was consistent with localization to the plasma membrane [Fig. 3, E and F; further supported by data from cauliflower mosaic virus (CaMV) 35S-SWEET-YFP plants, fig. S13]. AtSWEET11 and 12 were both expressed in select cells in the phloem, which form cell files along the veins (Fig. 3, C, D, and F, and fig. S12). Most likely, these cells correspond to phloem parenchyma. However, there are no known markers that would allow us to unambiguously identify these cells. Data from cell-specific translatome studies show that *AtSWEET11/12*-expressing cells have a clearly distinct translatome when compared to *SUC2*-expressing companion cells (fig. S6) (*17*). These data exclude the possibility that *SWEET11* and *12* are expressed to high levels in companion cells, supporting a localization in phloem parenchyma cells as the only remaining cell type in the phloem besides the enucleate sieve elements.

Further, *OsSWEET11/Xa13*, encoding a sucrose uniporter and functioning as a rice susceptibility (S) gene (*Xa13*) for specific pathovars of

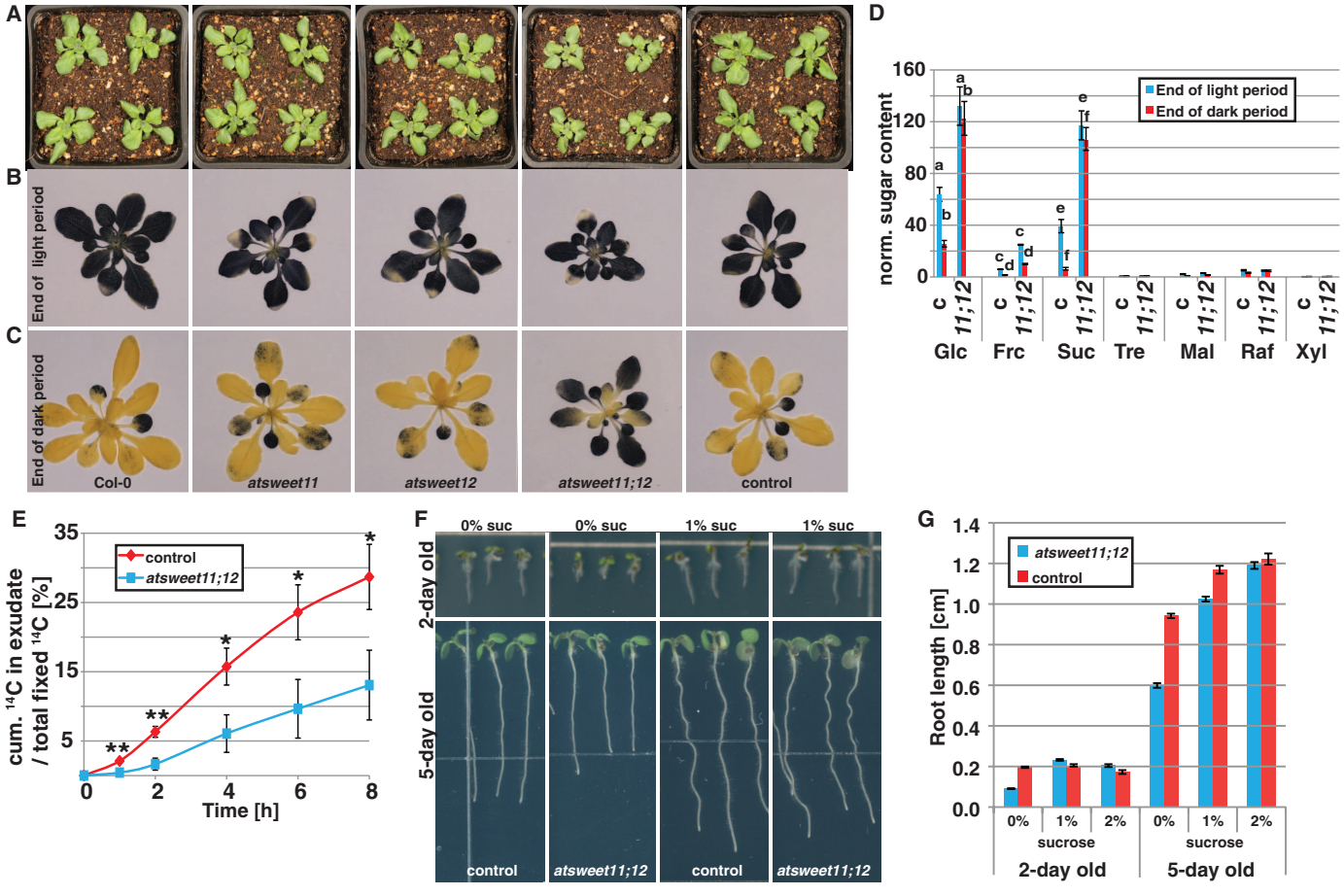

Fig. 2. Phenotypic characterization of AtSWEET11 and 12 mutants. (**A**) Reduced growth of the *atsweeet11;12* double mutant relative to Col-0 wild type and isogenic wild type (control). (**B** and **C**) Elevated starch accumulation in *atsweeet11;12* single and double mutants at the end of the light and dark periods (high light conditions). (**D**) Sugar levels in mature leaves at the end of the light and dark periods (±SEM, $n \geq 6$; identical letters indicate significance between pairs (daytime) according to *t* test ($P \leq 0.001$; high light conditions). Glc, glucose; Frc, fructose; Suc, sucrose; Tre, trehalose; Mal, maltose; Raf, raffinose; Xyl, xylose; c, control; *11;12*, *atsweet11;12*. (**E**) Cumulative exudation of [^{14}C]-derived assimilates from cut petioles of leaves fed with $^{14}CO_2$ (^{14}C in exudate shown as percentage in exudate plus exudate from the previous exudation period for each time point; ±SEM, $n = 5$; **t* significant at $P < 0.05$, ***t* significant at $P < 0.01$) (low light conditions). (**F** and **G**) Impaired root growth of *atsweet11;12* seedlings grown on sugar-free media and media supplemented with sucrose [±SEM, $n \geq 60$; two-way analysis of variance indicates a significant interaction ($P < 0.0001$) between genotype and sucrose treatment].

Xanthomonas oryzae pv. *oryzae*, was found to be expressed in the phloem of uninfected rice leaves (*23*), indicating that OsSWEET11 may play a similar role in phloem loading. Coimmunolocalization of SUT1/SUC2 and SWEET11/12 to an extent detectable by transmission electron microscopy will be required to unambiguously define the cell type in which the SWEETs are functioning.

Our findings are compatible with a model suggested by Geiger (*24*), in which sucrose moves symplasmically via plasmodesmata toward the phloem and then effluxes close to the site of apoplasmic loading (fig. S15). We predict that communication is needed to coordinate the efflux from phloem parenchyma with the uptake into the SE/CC to prevent spillover and limit the availability of nutrient resources for pathogens in the apoplasm of the leaf. Invertases and glucose/H^+ cotransporters that are induced during pathogen infection may serve in retrieval of sugars spilled at the infection site (*25*). It is tempting to speculate that sugar- and turgor-controlled regulatory mechanisms involved in post-phloem unloading may also apply to sucrose efflux in the phloem loading process (*26*, *27*). The availability of SWEET sucrose transporters, together with FRET sensors (*28*), provides valuable tools for studying the regulatory networks coordinating local and long-distance transport and metabolism.

Clade III SWEETs had previously been implicated as key targets of biotrophic pathogens. OsSWEET11 and 14 are co-opted during infection of rice by *Xanthomonas oryzae* pv. *oryzae* (Xoo) (*12*, *21*, *29*, *30*). Pathovar-specific effectors secreted by Xoo activate the transcription of clade III SWEET genes, and mutations in the effector binding sites in SWEET promoters lead to resistance to Xoo in a wide spectrum of rice lines (*21*, *29*–*31*). Our finding that these SWEETs are key elements of the phloem translocation machinery indicates that the pathogen retools a critical physiological function (i.e., a cellular sucrose efflux mechanism in the phloem) to gain access to the plant's energy resources at the site of infection.

However, this function is redundant in the plant. Such redundancy in both pathogen and host functions has been attributed to increased system robustness and may have evolved to allow the plant to survive mutations in essential functions that create pathogen resistance (*32*). It is possible that the highly localized transfer of sucrose between phloem parenchyma and SE/CC has evolved to limit sucrose release into the apoplasm to a limited interface of adjacent cells inside the phloem, and thus to reduce the availability of sucrose in the apoplasm to pathogens. Pathogens can overcome this first line of defense by targeting exactly this efflux mechanism in order to gain access to sugars in cells surrounding the infection site—for example, in the epidermis or mesophyll. Invertase and monosaccharide transporters, which are also typically induced during infection, may then serve as a secondary line of defense to reduce apoplasmic sugar levels at the infection site (*25*). The work presented here adds a crucial item to the list of machinery essential for carbon allocation: the transport proteins responsible for the efflux of sucrose to apoplasm in preparation for phloem loading.

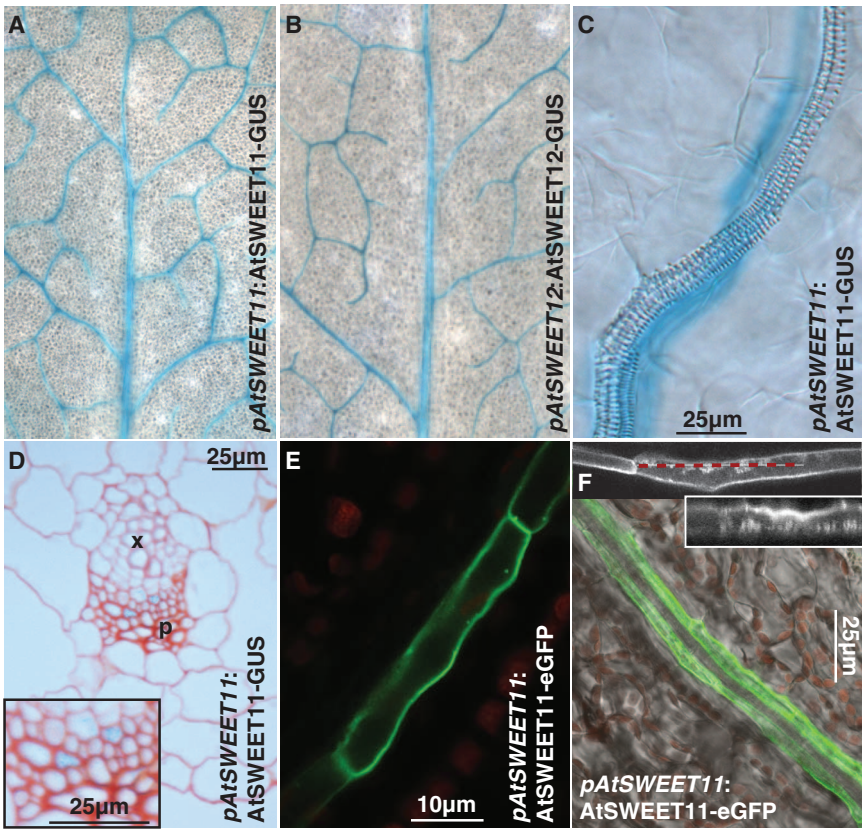

Fig. 3. GUS and eGFP localization of *AtSWEET11* and *12* promoter-reporter fusions. (**A** to **D**) GUS histochemistry analysis in rosette leaves of transgenic *Arabidopsis* plants expressing translational GUS fusions of *AtSWEET11* [(A), (C), and (D)] or 12 (B) from their native promoters. (A) and (B), GUS staining detected in leaf vein network; (C), high-resolution images of expression in one cell file of an individual vein; (D), cross section of *Arabidopsis* leaf showing cell-specific localization of AtSWEET11. (**E** and **F**) Confocal images of eGFP fluorescence in sepal vein cell files of transgenic *Arabidopsis* plants expressing translational AtSWEET11-eGFP fusions under control of its native promoter. Insets in (F) show eGFP channel in black and white; red dashed line in upper inset indicates position of *z*-scan shown in lower inset. eGFP accumulation is observed in static puncta, which may be caused by accumulation of AtSWEET11 in membranes in cell wall ingrowths, a characteristic feature of phloem parenchyma cells (*33*). The presence of cell wall ingrowth was confirmed by electron microscopy (fig. S14).

References and Notes

1. X. G. Zhu, S. P. Long, D. R. Ort, *Annu. Rev. Plant Biol.* **61**, 235 (2010).
2. A. H. Paterson, Z. K. Li, *Proc. Natl. Acad. Sci. U.S.A.* **108**, 10931 (2011).
3. S. Lalonde, D. Wipf, W. B. Frommer, *Annu. Rev. Plant Biol.* **55**, 341 (2004).
4. R. T. Giaquinta, *Annu. Rev. Plant Physiol.* **34**, 347 (1983).
5. B. G. Ayre, *Mol. Plant* **4**, 377 (2011).
6. Q. Fu, L. Cheng, Y. Guo, R. Turgeon, *Plant Physiol.* **157**, 1518 (2011).
7. J. W. Riesmeier, B. Hirner, W. B. Frommer, *Plant Cell* **5**, 1591 (1993).
8. J. W. Riesmeier, L. Willmitzer, W. B. Frommer, *EMBO J.* **11**, 4705 (1992).
9. J. W. Riesmeier, L. Willmitzer, W. B. Frommer, *EMBO J.* **13**, 1 (1994).
10. L. Bürkle *et al.*, *Plant Physiol.* **118**, 59 (1998).
11. J. R. Gottwald, P. J. Krysan, J. C. Young, R. F. Evert, M. R. Sussman, *Proc. Natl. Acad. Sci. U.S.A.* **97**, 13979 (2000).
12. L. Q. Chen *et al.*, *Nature* **468**, 527 (2010).
13. I. Lager, L. L. Looger, M. Hilpert, S. Lalonde, W. B. Frommer, *J. Biol. Chem.* **281**, 30875 (2006).
14. R. Lemoine, S. Delrot, *FEBS Lett.* **249**, 129 (1989).
15. J. W. Maynard, W. J. Lucas, *Plant Physiol.* **70**, 1436 (1982).
16. J. W. Yu *et al.*, *Mol. Cell* **13**, 677 (2004).
17. S. Santagata *et al.*, *Science* **292**, 2041 (2001).
18. D. Osuna *et al.*, *Plant J.* **49**, 463 (2007).
19. A. C. Srivastava, S. Ganesan, I. O. Ismail, B. G. Ayre, *Plant Physiol.* **148**, 200 (2008).
20. F. Rolland, E. Baena-Gonzalez, J. Sheen, *Annu. Rev. Plant Biol.* **57**, 675 (2006).
21. G. Antony *et al.*, *Plant Cell* **22**, 3864 (2010).
22. E. Haritatos, R. Medville, R. Turgeon, *Planta* **211**, 105 (2000).
23. Z. Chu *et al.*, *Theor. Appl. Genet.* **112**, 455 (2006).
24. D. R. Geiger, S. A. Sovonick, T. L. Shock, R. J. Fellows, *Plant Physiol.* **54**, 892 (1974).
25. P. N. Sutton, M. J. Gilbert, L. E. Williams, J. L. Hall, *Physiol. Plant.* **129**, 787 (2007).
26. J. W. Patrick, C. E. Offler, *J. Exp. Bot.* **52**, 551 (2001).
27. Y. Zhou *et al.*, *J. Exp. Bot.* **60**, 71 (2009).
28. S. Okumoto, H. Takanaga, W. B. Frommer, *New Phytol.* **180**, 271 (2008).

29. B. Yang, A. Sugio, F. F. White, *Proc. Natl. Acad. Sci. U.S.A.* **103**, 10503 (2006).
30. M. Yuan, Z. Chu, X. Li, C. Xu, S. Wang, *Plant Cell Physiol.* **50**, 947 (2009).
31. Z. Chu *et al.*, *Genes Dev.* **20**, 1250 (2006).
32. A. Lundby, H. Mutoh, D. Dimitrov, W. Akemann, T. Knöpfel, *PLoS ONE* **3**, e2514 (2008).
33. K. Ataka, V. A. Pieribone, *Biophys. J.* **82**, 509 (2002).

Acknowledgments: We thank G. Grossmann and D. Ehrhardt for advice and help with confocal imaging; J. Bailey-Serres for help with the translatome analyses; K. Barton and T. Liu for plastic embedding and sectioning help and advice; and V. Lanquar and A. Jones for critical reading of the manuscript. Supported by U.S. Department of Energy grant DE-FG02-04ER15542 and National Institute of Diabetes and Digestive and Kidney Diseases grant 1RO1DK079109 (W.B.F.); the Carnegie Institution and the Scholarship Program of the Chinese Scholarship Council (grant 2009635108) (X.-Q.Q.); and the Max-Planck-Gesellschaft (S.O. and A.R.F.). Author contributions: W.B.F. and L.-Q.C. conceived and designed the experiments. L.-Q.C., X.-Q.Q., D.S., B.-H.H., and S.O. performed the experiments. W.B.F., L.-Q.C., X.-Q.Q., D.S., B.-H.H., S.O., and A.R.F. analyzed the data. L.-Q.C. and W.B.F. wrote the manuscript.

Supporting Online Material
www.sciencemag.org/cgi/content/full/science.1213351/DC1
Materials and Methods
Figs. S1 to S15
References (*34*–*60*)

30 August 2011; accepted 8 November 2011
Published online 8 December 2011;
10.1126/science.1213351

Changes in Wind Pattern Alter Albatross Distribution and Life-History Traits

Henri Weimerskirch,[1]* Maite Louzao,[1,2]† Sophie de Grissac,[1] Karine Delord[1]

Westerly winds in the Southern Ocean have increased in intensity and moved poleward. Using long-term demographic and foraging records, we show that foraging range in wandering albatrosses has shifted poleward in conjunction with these changes in wind pattern, while their rates of travel and flight speeds have increased. Consequently, the duration of foraging trips has decreased, breeding success has improved, and birds have increased in mass by more than 1 kilogram. These positive consequences of climate change may be temporary if patterns of wind in the southern westerlies follow predicted climate change scenarios. This study stresses the importance of foraging performance as the key link between environmental changes and population processes.

The vast majority of studies of the effects of changing environments on species biology have been conducted in terrestrial ecosystems and temperature and rainfall have been the main environmental factors considered (*1*, *2*), potentially ignoring other key climatic variables. In marine systems, wind is a major component of the environment, and climate change–induced alterations in oceanic wind regimes and strength have already occurred (*3*) and are predicted to increase (*4*). For example, over the past 50 years, Southern Hemisphere westerlies have shifted poleward and increased in intensity following movement of the Southern Annular Mode (SAM, characterized as increased pressure between 40° and 65°S) into a positive phase (*5*, *6*). Such changes in wind regime may affect the movement or distribution of wind-dependent species, such as migratory land birds (*7*) or pelagic seabirds (*8*–*10*). Pelagic seabirds, in particular, are wide-ranging predators that rely extensively on wind to move at low costs between breeding and foraging sites (*8*, *11*), suggesting that they may be highly affected by wind pattern changes.

Here, we investigate whether changes in wind conditions over the Southern Ocean have influenced the foraging ecology and life-history traits of the wandering albatross (*Diomedea exulans*), one of the most wide-ranging pelagic seabirds. We aimed to assess whether the foraging performance of albatrosses has changed over the past few decades in relation to wind conditions and to understand the possible consequences of such change on life history (i.e., breeding performance and condition). We combine data on the duration of foraging trips and breeding success collected over nearly 40 years, from 1966 to 2010, as well as foraging performance and body mass (1989 to 2010) of breeders from Crozet Islands, located in the windiest area of the Southern Ocean.

In the western Indian Ocean sector of the Southern Ocean, wind speeds have increased in the center of the westerly flow (Fig. 1), as well as locally at Crozet (Fig. 2B), as a result of the shift of the global SAM index into a positive phase (Fig. 2A). No changes occurred in subtropical waters, whereas wind speed increased in sub-Antarctic waters, especially south of Crozet (table S1 and Fig. 1). When decomposing wind into its two components—zonal wind from west to east, and meridional wind from north to south (Fig. 1)—the most pronounced changes have occurred for the latter. The meridional component has strongly increased and shifted poleward, whereas these trends were not as strong for the zonal component (Figs. 1 and 2, C and D).

Crozet wandering albatrosses foraged from subtropical to Antarctic waters at a maximum range of more than 3500 km (Fig. 1, upper panels). Although both sexes overlap in the latitudinal band of 40° to 50°S, males prefer colder waters at the latitude of Crozet or to the south (down to 60°S), whereas females favor warmer waters to the north as far as 30°S (Fig. 1, lower panels). Foraging parameters estimated from tracking data have changed over the past 20 years in parallel to changes in wind conditions. The northern range (the most northerly latitude attained during a foraging trip) of wandering albatrosses was strongly influenced by meridional winds and shifted extensively poleward in females and to a smaller extent in males (Table 1 and Fig. 3), whereas there was no significant trend over time for the southern range (Table 1). Concurrently, there was a significant decrease in the maximum distance from the colony (Table 1, foraging range).

As shown by earlier studies (*8*, *11*), wind strongly influenced albatross flight speed. We found that the meridional component best explained the increase in flight speed during a foraging trip (Table 1). Flight speeds increased until 2008, whereas the last value of the time series (2010) was characterized by very low wind speeds, comparable to those in the early 1990s (Figs. 2 and 3). Travel speed (daily distance covered) increased in both sexes, in relation to wind speed, whereas total distance covered did not change (Table 1 and Fig. 3). Females spent a higher proportion of the overall foraging time in flight than males (Fig. 3). Thus, the increase in the daily distance covered was due, for females, to an increase in flight speed with a concomitant shift in distribution poleward into more windy conditions, whereas for males it was due to shorter time periods spent sitting on the water.

Even though the total distance covered did not increase over years, the duration of foraging trips decreased due to increasing meridional winds (Table 1). This decrease in the duration of trips was confirmed over a longer period (during the past 4 decades; in 1970, 1989, 1999, and 2008) from an independent large data set: The mean duration of foraging trips was highly variable (2 to 35 days), similar between sexes, and decreased by 22% between 1970 and 2008 (from 12.4 ± 6.8 to 9.7 ± 5.5 days; fig. S1, mixed effect analysis of variance, year effect $F_{3,724} = 11.3$, $P < 0.001$). Finally, the angle between flight direction and wind direction shifted by 10° from 1989 to 2010, with birds tending to use tail winds to a larger extent in the 1990s than in the 2000s (fig. S2).

[1]Centre d'Etudes Biologiques de Chizé, CNRS, 79360 Villiers en Bois, France. [2]Helmholtz Centre for Environmental Research, Permoserstrasse 15, 04318 Leipzig, Germany.

*To whom correspondence should be addressed. E-mail: henriw@cebc.cnrs.fr

†Present address: Instituto Español de Oceanografía, CO Xixón, Camín de l'Arbeyal s/n, 33212 Xixón, Spain.